

## Quantum Effects in the Differential Cross Sections for the Insertion Reaction $N(^2D) + H_2$

Nadia Balucani,<sup>1</sup> Laura Cartechini,<sup>1</sup> Giovanni Capozza,<sup>1</sup> Enrico Segoloni,<sup>1</sup> Piergiorgio Casavecchia,<sup>1</sup> Gian Gualberto Volpi,<sup>1</sup> F. Javier Aoiz,<sup>2</sup> Luis Bañares,<sup>2</sup> Pascal Honvault,<sup>3</sup> and Jean-Michel Launay<sup>3</sup>

<sup>1</sup>*Dipartimento di Chimica, Università di Perugia, 06123 Perugia, Italy*

<sup>2</sup>*Departamento de Química Física, Universidad Complutense, 28040 Madrid, Spain*

<sup>3</sup>*PALMS, UMR 6627 du CNRS, Université de Rennes 1, Campus de Beaulieu, 35042 Rennes Cedex, France*

(Received 26 February 2002; published 13 June 2002)

The quantum (QM) scattering theory has been difficult to apply to the family of insertion reactions and the approximate quasiclassical trajectory (QCT) method or statistical calculations were mostly applied. In this Letter, we compare the experimental differential cross sections for the title insertion reaction with the results of QM and QCT calculations on an *ab initio* potential energy surface. The QM results reproduce well the crossed beam experiment, while a small, but significant, difference in the QCT ones points to quantum effects, possibly the occurrence of tunneling through the combined potential and centrifugal barrier.

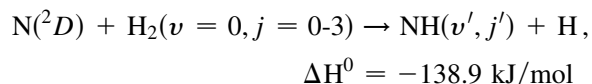
DOI: 10.1103/PhysRevLett.89.013201

PACS numbers: 34.50.Lf, 82.20.Ej, 82.20.Xr

The interaction between experiment and theory, fundamental in any scientific field, has proved to be indispensable for the progress of the field of reaction dynamics. Only the direct comparison between detailed experimental observables, such as the differential cross section (DCS), and quantum scattering calculations can indeed assess the quality of a computed potential energy surface (PES) and, in turn, allow the knowledge of the factors which determine and describe the behavior of a reactive system. Such an ambitious task has been accomplished only for a few simple reactions and, in all cases, the comparison between experimental results and accurate quantum scattering calculations led to a refinement of the *ab initio* calculated PESs. The three benchmark systems which have attracted the largest effort in the last decades, i.e.,  $H + H_2$ ,  $F + H_2$ , and  $Cl + H_2$ , all belong to the same class of *abstraction* reactions (for a recent review, see Ref. [1]). Only more recently a new effort has been directed toward the combined experimental and theoretical investigation of the more complex family of *insertion* reactions, which usually involve electronically excited atoms—such as the important species  $O(^1D)$ —and occur on multiple potential energy surfaces [2,3]. The reaction  $O(^1D) + H_2 \rightarrow OH + H$  has long served as the prototypical insertion reaction, but other systems such as  $C(^1D) + H_2$ ,  $S(^1D) + H_2$  and the title reaction have recently added to the list of simple systems for which DCSs have been measured [4–6] and PESs have become available [7–9]. The common characteristic of these reactions is that they occur on PESs with a deep potential well between reactants and products, associated with a strongly bound species ( $H_2O$ ,  $CH_2$ ,  $H_2S$ , and  $NH_2$ ) which is formed following the insertion of the excited atom into the H-H bond. Because of the presence of a very deep well (of the order of a few eV), the wave function has to be expanded on a very large number of states. This makes accurate quantum (QM) calculations quite arduous

and most of the time-independent QM codes have been applied only to direct abstraction reactions. Until very recently, when a method using body-frame democratic hyperspherical coordinates [10] has revealed to be suitable for the treatment of insertion reactions [3,11,12], only approximate methods, such as quasiclassical trajectory (QCT) or reduced dimensionality QM calculations were available together with time-dependent QM calculations—which, however, did not produce DCSs. Also a number of statistical studies are available, since insertion reactions are generally believed to proceed statistically because of the stability of the intermediate complex with respect to reactants and products. Nevertheless, as it was largely shown, the formation of a light, highly excited intermediate complex with few internal degrees of freedom seems to alter this simplistic prediction, and to address the statistical character of these reactions we have to rely on exact QM calculations on accurate PESs [4,13,14].

In this Letter we report a combined experimental and theoretical study on the insertion reaction



at a collision energy ( $E_c$ ) of 15.9 kJ/mol. Specifically, by carrying out crossed molecular beam (CMB) experiments we have derived reactive DCSs and by using both QM and QCT methods we have computed the reactive dynamics on a recently developed ground state  $1^2A''$   $NH_2$  PES [9]. The stimulus for the present work arises from the singular opportunity to compare experimental DCSs with those derived by an accurate QM treatment and by the widely used QCT method. As it is shown below, while the QCT calculations are able to predict only partly the shape of the DCSs, the QM predictions reproduce the experimental results over the explored angular range and thus assess the

good quality of the  $1^2A''$  PES and its ability to describe the reactive system at this  $E_c$ .

The experiments were performed using a CMB apparatus with mass spectrometric detection and product time-of-flight (TOF) analysis [15]. The experimental setup is similar to that described in a previous paper on the isotopic variant  $^{15}\text{N}(^2D) + \text{D}_2$  [6]. The extension to the reaction with  $\text{H}_2$ , necessary in order to perform the direct comparison with the QM results [16], has not been trivial. The previous choice of isotopes was dictated by the intent to avoid the interference from the nonreactively scattered  $^{15}\text{N}$ , present in the primary beam with its natural isotopic abundance, and to avoid the detection of the unfavorable mass-to-charge ratio  $m/e$  of 16. In the present case, in order to derive the DCSs for the  $\text{N}(^2D) + \text{H}_2$  reaction we have been forced to perform accurate measurements of the laboratory distributions at  $m/e = 15$ , due to both reactive scattering signal and elastic scattering of the isotope  $^{15}\text{N}$ , and at  $m/e = 14$ , so that, by using the right density ratio  $d^{15}\text{N}/d^{14}\text{N}$ , we have been able to evaluate and subtract the elastic contribution from the elastic + reactive distributions [17]. The characteristics of the radio frequency discharge source used to produce continuous beams of atomic nitrogen are given in Ref. [6]. For the present experiment beam velocity and speed ratio were 2860 m/s and 6.0, respectively. The  $\text{H}_2$  beam was produced by expanding neat  $\text{H}_2$  through a nozzle resistively heated at 440 K; as a consequence, the relative rotational state populations are 0.142, 0.590, 0.123, and 0.128 for  $j = 0, 1, 2$ , and 3, respectively, according to the experimental determination of Pollard *et al.* for a beam obtained under similar expansion conditions [18]. Peak velocity and speed ratio were 3160 m/s and 12.0, respectively. The measured laboratory angular distribution is reported in Fig. 1. The TOF spectra, also measured in our experiment, are not reported here and will be shown in a future paper.

QM reactive scattering calculations for an initial rovibrational state ( $v = 0, j = 0$ ) of  $\text{H}_2$  at  $E_c = 15.9$  kJ/mol have already been reported [11]. In the present work, we have extended these calculations to initial  $\text{H}_2$  states  $v = 0,$

$j = 1, 2$  so that a comparison with the experiment is possible. Briefly stated, we use a time-independent method which employs body-frame democratic hyperspherical coordinates [10]. At each hyperradius  $\rho$ , we compute a set of eigenstates of a reference Hamiltonian. The nuclear scattering wave function is expanded on these eigenstates which dissociate at large  $\rho$  into the  $\text{H}_2$  (12, 8, 3) and  $\text{NH}$  (35, 32, 30, 27, 24, 20, 16, 11) rovibrational sets (this notation indicates the largest rotational level  $j$  for each vibrational manifold). The coefficients of the expansion satisfy a set of second order coupled differential equations with couplings arising from the difference between the exact Hamiltonian and the reference Hamiltonian. No restrictions were placed on the helicity quantum number  $\Omega$  (the projection of the total angular momentum  $J$  of the system on each of the atom-diatom axes). Thus,  $\Omega_{\text{max}} = J$  and the number of coupled equations increases from 215 for  $J = 0$  to 2917 for  $J = 26$ . In order to simulate the laboratory distributions, it would be necessary to derive the DCS also for initial  $j = 3$ . Such a calculation implies a very large computer time and was not performed because it was observed that at the lower  $E_c$  of 8.8 kJ/mol (where scattering calculations are less expensive) the DCS for initial  $j = 3$  is similar to that of  $j = 2$ , so that we can assume that the DCS for initial  $j = 2$  and 3 are also the same at 15.9 kJ/mol. The DCSs for the three initial  $j$ 's are shown in Fig. 2. We also derived the final product internal energy distributions (not shown here) because their complement, i.e., the translational energy distributions, are necessary to simulate the laboratory distributions.

With the aim to directly compare QM and experimental results with the predictions of the QCT method, we have performed QCT calculations by running a batch of 200 000 trajectories at  $E_c = 15.9$  kJ/mol and  $\text{H}_2(v = 0, j = 0-3)$  following the procedures described elsewhere [19]. The QCT DCSs are also shown in Fig. 2. Although the agreement between QM and QCT DCSs improves with increasing initial  $j$ , significant discrepancies are visible especially for  $j = 0$  and 1. In particular, while the

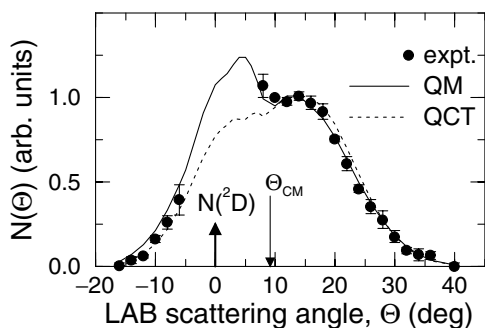


FIG. 1. Experimental  $\text{NH}$  laboratory angular distribution at  $E_c = 15.9$  kJ/mol (solid circles; the standard deviations are also shown) and QM (solid line) and QCT (dashed line) predictions (see text).

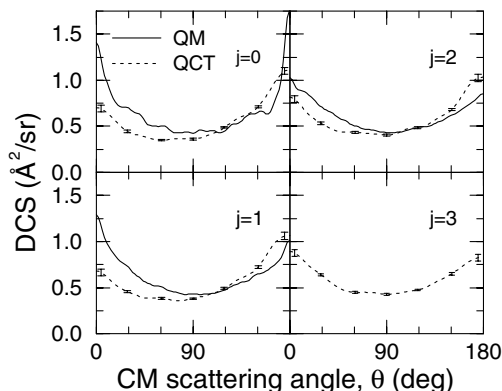


FIG. 2. QM (solid lines) and QCT (dashed lines) CM DCSs for the different initial  $j$  of  $\text{H}_2$  relevant in the crossed beam experiment.

QCT DCSs show a preference for backward scattering, the QM ones show an alternating behavior with the DCS for  $j = 0$  slightly favoring backward scattering ( $\theta = 180^\circ$ ) and the DCSs for  $j = 1$  and 2 favoring forward scattering ( $\theta = 0^\circ$ ). In all cases, the QCT calculations are seen to underestimate the QM intensity in the forward hemisphere. As far as the product energy release is concerned, QM and QCT predictions are in very good agreement.

In order to compare the theoretical results with the measured angular distribution in the most straightforward way, we have transformed the theoretical DCSs derived in the center-of-mass (CM) frame into the laboratory (LAB) frame, taking into consideration the averaging over the experimental conditions (beam velocity distributions and angular divergences, detector aperture) and the distribution of  $j$ 's and their relative reactivity. Also, the translational energy distributions as they were derived from QM and QCT calculations for each initial  $j$  were used in the simulation. The results are shown in Fig. 1 together with the experimental results. As can be appreciated, the QM calculations are able to reproduce the shape of the experimental distribution giving the right intensity ratios between the innermost available angle ( $\Theta = 8^\circ$ ) and all the others. On the other hand, the QCT ones underestimate the intensity of the products scattered on the left of the CM velocity vector, corresponding to the forward direction in the CM frame, and overestimate the intensity of the products on the right (backward direction). For instance, the experimental intensity ratio  $I(\Theta = 8^\circ)/I(\Theta = 16^\circ)$  is 1.10, while the QM and QCT ones are 1.05 and 0.89, respectively (the latter being well outside the experimental uncertainty). The situation was analogous in the case of the previously studied  $N(^2D) + D_2$  reaction [6], in which the LAB angular distributions were compared with QCT calculations on the same PES at two different  $E_c$ . In both cases, the QCT results underestimated the intensity in the forward direction and overestimated that in the backward direction. We recall that in the case of  $N(^2D) + D_2$ , the more friendly kinematics allowed a better determination of the peak in the forward direction, which is, instead, partly obscured in the present experiment by the "blind" angular range close to  $\Theta = 0^\circ$  where the detector cannot be placed.

Once ascertained that the differences between QM and QCT results are evident also in the LAB frame and that the QM calculations are able to reproduce overall the experimental distributions better than the QCT ones, it is important to understand the reason for such a difference. Being the two kinds of calculations performed on the same PES, an obvious conclusion is that the differences are due to the limitations of the QCT method. To understand the origin of the discrepancies, we have analyzed the QM and QCT reaction probabilities as a function of orbital angular momentum  $L$  and the QM and QCT DCSs as they change with the maximum value of the angular momentum,  $L_{\max}$ , considered. Figure 3(a) shows the QM and QCT total  $(2L + 1)$  degeneracy-weighted) reaction probabilities as a function

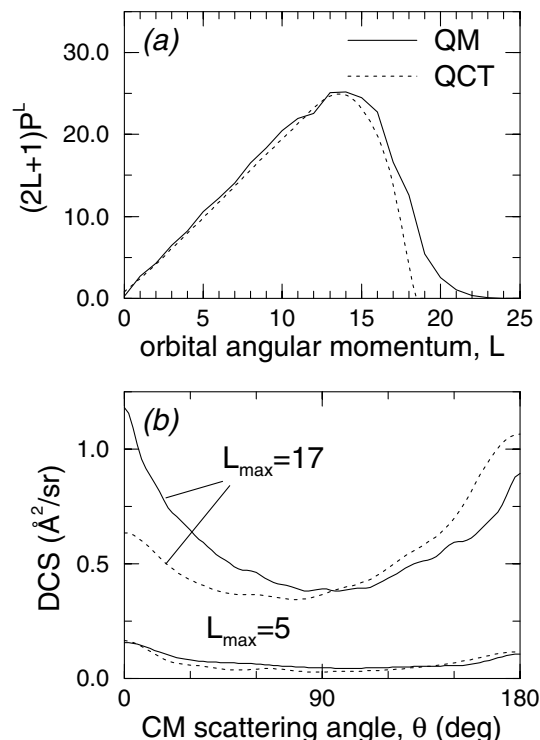


FIG. 3. (a) QM and QCT total  $(2L + 1)$  degeneracy-weighted) reaction probabilities as a function of the orbital angular momentum  $L$  for the  $N(^2D) + H_2(v = 0, j = 1)$  reaction, and (b) DCSs as a function of the maximum orbital angular momentum  $L_{\max}$  retained in the partial wave sum.

of  $L$ , while in Fig. 3(b) the QM and QCT DCSs are shown for two different values of  $L_{\max}$ . The two plots are for the reaction with initial  $j = 1$  since this is the dominant contribution in the scattering experiment; in any case, the same behavior has been observed when considering the reaction of initial  $j = 0$ . It is apparent from Fig. 3(a) that the QM reaction probability extends to values of  $L$  higher than the QCT one. If the reaction under study were a direct reaction, being in that case the forward scattering associated with large angular momenta (or, in classical mechanics, with large impact parameters) the increased reactivity of larger  $L$  could directly account for the differences in the QM and QCT treatment. Unfortunately, if we analyze the DCSs as they change with the considered  $L_{\max}$ , a complication arises from the fact that, being  $N(^2D) + H_2$  an indirect reaction, the correlation small/large impact parameters-backward/forward scattering is not as valid as for a direct reaction. As a matter of fact, all the impact parameters (and consequently all values of  $L$ ) contribute to generate intensity in the whole angular range. Nevertheless, some considerations can still be made. The QM and QCT DCSs averaged over small values of  $L_{\max}$  [see Fig. 3(b) for  $L_{\max} = 5$ ] are essentially coincident and slightly forward biased. However, at higher values of  $L_{\max}$ , a clear difference becomes visible. In Fig. 3(b), the QM and QCT DCSs for  $L_{\max} = 17$  are also shown: while the

QCT DCS has progressively shifted towards a backward biased function, the QM one has reinforced the preference for forward scattering, thus confirming the role of higher  $L$  in generating the forward scattering seen in the QM case. Interestingly, a similar behavior has been seen for the insertion reaction  $O(^1D) + H_2$  [20]. We recall that also in the case of the abstraction reaction  $F(^2P) + H_2$ , QM calculations on a recent PES systematically found more intensity in the forward direction with respect to QCT calculations [21]. A similar analysis of the reaction probabilities and of the DCSs as they change with the value of  $L_{\max}$  was performed and the authors suggested that tunneling through the combined potential and centrifugal barrier for large values of  $L$  could be responsible for what is observed in  $F + H_2$ . In view of the present analysis, we can also consider the tunneling through the combined potential ( $\sim 8$  kJ/mol) and centrifugal barrier as one of the possible causes of the discrepancies found between QM and QCT DCSs at large values of  $L$ . At small values of  $L$ , the effect of the centrifugal barrier is also small and, being the collision energy larger than the potential barrier, the differences between QM and QCT are expected to be minor as in fact they are. For the final assessment of this quantum effect, however, further analysis is in progress, also relatively to the system  $O(^1D) + H_2$ .

A final remark needs to be made about the value of the reaction rate constant at 300 K, which has been found to be lower than the experimental one in the present QCT calculations ( $1.90 \times 10^{-12}$  cm<sup>3</sup>/s), while QM calculations predict a value of  $2.51 \times 10^{-12}$  cm<sup>3</sup>/s, in very good agreement with the experimental determination of  $2.44 \pm 0.34 \times 10^{-12}$  cm<sup>3</sup>/s [22].

In summary, the present comparison between experimental DCS and QM/QCT calculations appears to sustain the accuracy of the recently derived  $NH_2$  ground state potential energy surface. Also, there is no need to invoke a contribution from the first excited surface, either in reproducing dynamical measurements or the rate constants, as it was previously suggested [6,9]. Another interesting conclusion is that the discrepancies found between the QCT and QM calculations suggest that the same quantum effects already seen for other reactions are present for the class of insertion reactions as well.

N.B. acknowledges fruitful discussions with D. Skouteris and A. Laganà. This work has been supported by MIUR (COFIN 2001) of Italy, DGES of Spain (PB98-0762-C03-01), the European Commission within the RT Network *Reaction Dynamics* (Contract No. HPRN-CT-1999-00007), and the Italian-Spanish Scientific Program *Acciones Integradas* (HI1999-0081). The QM dynamical calculations were performed on a NEC-SX5 vector supercomputer, through a grant from the Institut du Développement et des Ressources en Informatique Scientifique (IDRIS) in Orsay (France).

- [1] P. Casavecchia, Rep. Prog. Phys. **63**, 355 (2000).
- [2] X. Liu, J.J. Lin, S. Harich, G.C. Schatz, and X. Yang, Science **289**, 1536 (2000).
- [3] F.J. Aoiz, L. Bañares, J.F. Castillo, M. Brouard, W. Denzer, C. Vallance, P. Honvault, J.-M. Launay, A.J. Dobbyn, and P.J. Knowles, Phys. Rev. Lett. **86**, 1729 (2001).
- [4] A. Bergeat, L. Cartechini, N. Balucani, G. Capozza, L.F. Phillips, P. Casavecchia, G.G. Volpi, L. Bonnet, and J.-C. Rayez, Chem. Phys. Lett. **327**, 197 (2000).
- [5] S.-H. Lee and K. Liu, J. Phys. Chem. A **102**, 8637 (1998).
- [6] N. Balucani, M. Alagia, L. Cartechini, P. Casavecchia, G.G. Volpi, L.A. Pederson, and G.C. Schatz, J. Phys. Chem. A **105**, 2414 (2001).
- [7] B. Bussery-Honvault, P. Honvault, and J.-M. Launay, J. Chem. Phys. **115**, 10701 (2001).
- [8] A. S. Zyubin, A. M. Mebel, S. D. Chao, and R. T. Skodje, J. Chem. Phys. **114**, 320 (2001).
- [9] L. A. Pederson, G. C. Schatz, T.-S. Ho, T. Hollebeek, H. Rabitz, L. B. Harding, and G. Lendvay, J. Chem. Phys. **110**, 9091 (1999).
- [10] J.-M. Launay and M. Le Dourneuf, Chem. Phys. Lett. **163**, 178 (1989).
- [11] P. Honvault and J.-M. Launay, J. Chem. Phys. **111**, 6665 (1999).
- [12] P. Honvault and J.-M. Launay, J. Chem. Phys. **114**, 1057 (2001).
- [13] P. Honvault and J.-M. Launay, Chem. Phys. Lett. **329**, 233 (2000).
- [14] E. J. Rackham, F. Huarte-Larranaga, and D. E. Manolopoulos, Chem. Phys. Lett. **343**, 356 (2001).
- [15] M. Alagia, N. Balucani, P. Casavecchia, D. Stranges, and G. G. Volpi, J. Chem. Soc. Faraday Trans. **91**, 575 (1995).
- [16] When considering the isotopic variant  $N(^2D) + D_2$ , the largely increased number of states make the QM calculations extremely computer time consuming.
- [17] Both <sup>15</sup>N and <sup>14</sup>N are produced in the beam source from dissociation of molecular nitrogen (see [6]), with the same velocity and beam characteristics. Because of the very little difference in mass, the elastic scattering properties of the two isotopes are about the same and the two laboratory elastic distributions can be assumed identical. We also verified this assumption by scattering the same nitrogen beam from He.
- [18] J.E. Pollard, D.J. Trevor, Y.T. Lee, and D.A. Shirley, J. Chem. Phys. **77**, 4818 (1982).
- [19] F.J. Aoiz, L. Bañares, and V.J. Herrero, J. Chem. Soc. Faraday Trans. **94**, 2483 (1998).
- [20] P. Honvault, J.-M. Launay, F.J. Aoiz, and L. Bañares (to be published).
- [21] J.F. Castillo, D.E. Manolopoulos, K. Stark, and H.-J. Werner, J. Chem. Phys. **104**, 6531 (1996).
- [22] T. Suzuki, Y. Shihira, T. Dato, H. Umemoto, and S. Tsunashima, J. Chem. Soc. Faraday Trans. **89**, 995 (1993).